

Preparation and characterization of Fe/MgO catalysts obtained from hydrotalcite-like compounds

Jianyi Shen ^{*}, Bing Guang, Mai Tu, Yi Chen

Department of Chemistry, Nanjing University, Nanjing 210093, China

Abstract

Iron–magnesium hydrotalcite-like compounds with Mg/Fe ratios from 1 to 10 were synthesized by using an $\text{NH}_4\text{OH}/(\text{NH}_4)_2\text{CO}_3$ solution as the precipitation agent. TG–DTA results showed that the decomposition of the samples proceeds in two stages at temperatures around 505 and 640 K, corresponding to the sequential loss of interlayer water, and hydroxide and carbonate groups. After calcination at 673 K, these samples are transformed into Fe–Mg mixed oxides with high surface areas around $200 \text{ m}^2/\text{g}$ and mesopores around 15 nm in diameter. The results of temperature-programmed reduction and Mössbauer spectroscopy revealed that the reduction of the calcined Fe–Mg HTLC samples proceeds in two steps from Fe^{3+} to $\alpha\text{-Fe}$ through Fe^{2+} . While the pure iron sample was completely reduced to $\alpha\text{-Fe}$ at 673 K, less than 60% of iron species in the calcined Fe–Mg HTLC samples were reduced to $\alpha\text{-Fe}$ at 773 K. The catalysts prepared from Fe–Mg HTLC exhibited lower CO conversion and much higher selectivity to CO_2 as compared to the pure iron catalyst in the Fischer–Tropsch reaction.

Keywords: Iron–magnesium hydrotalcite; Iron–magnesium mixed oxides; Fe/MgO catalysts; Fischer–Tropsch synthesis; Mössbauer spectroscopy

1. Introduction

Hydrotalcite-like compounds (HTLC) consist of brucite-like layers containing octahedrally coordinated bivalent and trivalent cations as well as interlayer anions and water [1–4]. Because of the many applications as adsorbents, catalysts and catalyst supports, HTLC have received much attention in recent years [5–17]. It was reported that highly dispersed metal catalysts can be prepared by using HTLC as precursors [3,13,14]. However, little work has been

done concerning the Fe/MgO catalysts obtained from Fe–Mg HTLC. In this work, we synthesized Fe–Mg HTLC following the method described by Shen et al. [18] for the preparation of Al–Mg HTLC. The synthesized Fe–Mg HTLC were decomposed into Fe–Mg mixed oxides which were further reduced to Fe/MgO catalysts. The properties of the Fe–Mg HTLC, Fe–Mg mixed oxides and Fe/MgO catalysts were characterized by X-ray diffraction (XRD), TG–DTA (thermogravimetric and differential thermal analysis), transmission electron microscopy (TEM) and Mössbauer spectroscopy, etc. The Fe/MgO catalysts were found to exhibit special behavior in the Fischer–Tropsch reaction.

^{*} Corresponding author.

2. Experimental

HTLC samples with Mg/Fe ratios of 1, 2, 3, 6 and 10 were prepared. In each batch, $\text{Mg}(\text{NO}_3)_2 \cdot 6\text{H}_2\text{O}$ (AR) and $\text{Fe}(\text{NO}_3)_3 \cdot 9\text{H}_2\text{O}$ (AR) were mixed to obtain the desired ratio and were dissolved to obtain an aqueous solution of 230 ml with total cation concentrations of 1 M. NH_4OH (AR) and $(\text{NH}_4)_2\text{CO}_3$ (AR) were dissolved in deionized water to form another aqueous solution of 350 ml with appropriate amount calculated according to the relations of $[\text{NH}_4\text{OH}] = 2.2 [\text{Mg}^{2+}] + 3.2 [\text{Fe}^{3+}]$ and $[\text{CO}_3^{2-}] = 0.5 [\text{Fe}^{3+}]$. Then, the two solutions were added dropwise into 250 ml deionized water at 313 K in a 1000 ml beaker over an interval of 30 min, during which time a brown precipitate was formed. The pH of the slurry was controlled in the range of 8 to 9 by adding the two solutions alternately. After the two solutions were completely added, the slurry was stirred for another 30 min at 313 K. The precipitate formed was then filtered, washed with deionized water and usually dried at 393 K. The sample with the Mg/Fe ratio of n was designated as $n\text{Mg/Fe}$. For comparison, pure $\text{Fe}(\text{OH})_3$ and $\text{Mg}(\text{OH})_2$ were prepared in a similar manner.

The structure of the samples before and after calcination were determined by a Shimadzu XD-3A X-ray diffractometer using an iron source. TG-DTA was performed on a Rigaku thermal analyzer with the range of 10 mV, heating rate of 20 K/min and chart speed of 2.5 mm/min. The temperature for the calcination of the samples was selected according to the TG-DTA results. The surface areas and inner pore sizes of the calcined samples were measured by N_2 adsorption on a Micromeritics ASAP 2000. The samples were heat treated at 623 K and evacuated to 4×10^{-3} Torr before the BET measurements. Mössbauer spectra were collected at room temperature using a constant acceleration spectrometer equipped with a $^{57}\text{Co/Pd}$ source. The velocity scale of the spectrometer was calibrated with the ^{57}Fe Mössbauer

resonance. Isomer shifts are reported relative to $\alpha\text{-Fe}$. All iron species are supposed to have the same recoilless fraction to calculate the relative amount of different iron species in the samples according to their relative peak areas. Temperature-programmed reduction (TPR) of the calcined samples was performed by using a mixed gas with 5% H_2 in Ar and the heating rate of 16 K/min. The reduction properties were also studied by heating the samples in H_2 at constant temperatures followed by the phase determination with Mössbauer spectroscopy. Fischer-Tropsch reaction was performed in a microreactor connected to a gas-phase chromatograph equipped with a Propak-QS column. About 1 ml catalyst was loaded in an U-quartz reactor. The catalyst was pre-reduced in H_2 at 773 K for 4 h. The reaction was carried out at 593 K in atmospheric pressure. The syngas with H_2/CO ratio of 2 passed through the catalyst with the space velocity of 1000 h^{-1} .

3. Results and discussion

Fig. 1 shows the XRD patterns of the samples before calcination. All the samples with Mg/Fe ratios from 1 to 10 exhibited the diffraction patterns characteristic of the hydrotalcite-like structure [12], which is different from those

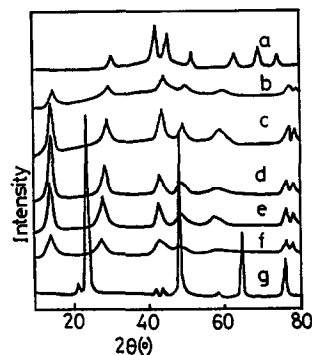


Fig. 1. XRD patterns of the synthesized iron, iron–magnesium and magnesium samples after being dried: (a) Fe_2O_3 , (b) 1Mg/Fe, (c) 2Mg/Fe, (d) 3Mg/Fe, (e) 6Mg/Fe, (f) 10Mg/Fe and (g) $\text{Mg}(\text{OH})_2$. The Fe_2O_3 sample was dried at 413 K. The other samples were dried at 393 K.

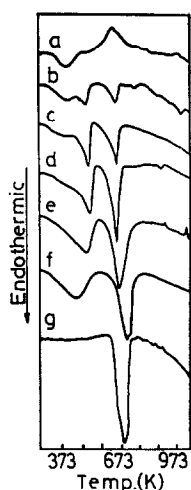


Fig. 2. DTA profiles of the synthesized iron, iron–magnesium and magnesium samples after being dried: (a) Fe_2O_3 , (b) 1Mg/Fe, (c) 2Mg/Fe, (d) 3Mg/Fe, (e) 6Mg/Fe, (f) 10Mg/Fe and (g) $\text{Mg}(\text{OH})_2$. The Fe_2O_3 sample was dried at 413 K. The other samples were dried at 393 K.

of Fe_2O_3 and MgO as also shown in Fig. 1 for comparison. However, the intensity of the XRD profiles of the samples with extreme Mg/Fe ratios, i.e., 1 and 10, was relatively lower than that of other samples. The DTA profiles of these samples are shown in Fig. 2. It is seen that all Fe–Mg HTLC exhibit similar DTA profiles with two endothermic peaks around 473 K and 673 K, confirming the formation of Fe–Mg HTLC. The two pure samples, Fe_2O_3 and $\text{Mg}(\text{OH})_2$ exhibited totally different features of the DTA profiles. A peak appeared around 373 K on the DTA profiles of the sample with the Mg/Fe ratio of 1 and the pure iron sample, indicating that some iron oxides might be contained in the 1 Mg–Fe HTLC sample.

To understand the decomposition procedure of the Fe–Mg HTLC samples, the TG–DTA profile of the 3Mg/Fe sample was analyzed in detail. As shown in Fig. 3, two weight loss stages can be observed on the TG curve, corresponding to the two endothermic peaks around 505 and 640 K on the DTA profile, demonstrating that the decomposition proceeded in two steps. When 15.56 mg sample was used, the total weight loss was found to be 6.55 mg, in which 2.20 mg was lost in the first step while

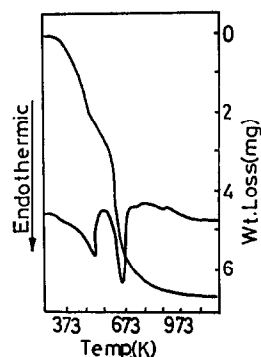


Fig. 3. TG–DTA curves for the 3Mg/Fe sample dried at 393 K.

4.35 mg was lost in the second step. Suppose that the initial sample has the composition of $\text{Mg}_6\text{Fe}_2(\text{OH})_{16}\text{CO}_3 \cdot x\text{H}_2\text{O}$ and that the final mixed oxide has the composition of $6\text{MgO} \cdot \text{Fe}_2\text{O}_3$, the formula weight of the initial sample can then be calculated to be 690.8 and the number of water molecules contained in the interlayer was found to be 5.7, which is approximately equal to 6. Thus, the formula of the 3Mg/Fe HTLC may be $\text{Mg}_6\text{Fe}_2(\text{OH})_{16}\text{CO}_3 \cdot 6\text{H}_2\text{O}$. Fig. 3 also shows that the sample loses water molecules around 505 K and hydroxide and carbonate groups around 640 K upon heat treatment. With these results, we calcined the Fe–Mg HTLC samples for 6 h at 673 K to remove all water, hydroxide and carbonate groups to produce Fe–Mg mixed oxides.

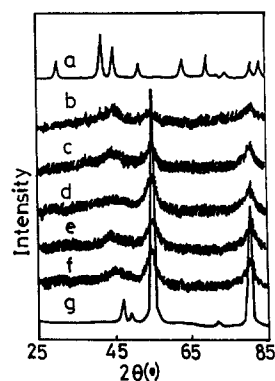


Fig. 4. XRD patterns of the synthesized iron, iron–magnesium and magnesium samples after calcination: (a) Fe_2O_3 , (b) 1Mg/Fe, (c) 2Mg/Fe, (d) 3Mg/Fe, (e) 6Mg/Fe, (f) 10Mg/Fe and (g) MgO. The MgO was obtained from $\text{Mg}(\text{OH})_2$ calcined at 773 K. The other samples were calcined at 673 K.

Table 1
BET surface areas of different samples after calcination

Sample	Fe ₂ O ₃	1Mg/Fe	3Mg/Fe	6Mg/Fe	MgO
BET area (m ² /g)	35	200	218	203	340

The X-ray diffraction patterns of the calcined samples are shown in Fig. 4. Three broad peaks with d values around 1.45, 2.05 and 2.55 can be observed for all the calcined Fe–Mg HTLC samples. The peaks with the d values of 1.45 and 2.05 can be assigned to MgO, while the peak with the d value of 2.55 may result from Fe₂O₃ ($d = 2.52$) or MgFeO₄ ($d = 2.53$). The BET surface areas of some calcined Fe–Mg HTLC samples as well as the Fe₂O₃ and MgO are given in Table 1. It is interesting that the calcined Fe–Mg HTLC samples had similar large surface areas around 200 m²/g. About 94% volume of pores had a diameter around 15 nm for the 3Mg/Fe sample after calcination.

Fig. 5 shows the Mössbauer spectra of the 3Mg/Fe sample. The HTLC sample displays a doublet of Fe³⁺ (IS = 0.34 mm/s) with quadruple splitting of 0.5 mm/s. After calcination at 673 K, the sample exhibits a doublet of Fe³⁺ (IS = 0.28 mm/s) with quadruple splitting of

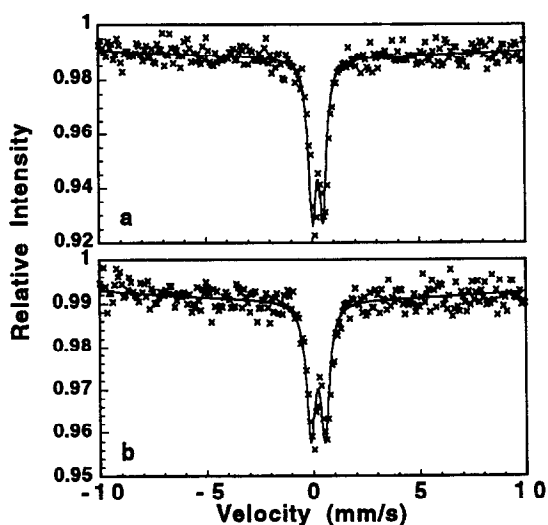


Fig. 5. Mössbauer spectra of the 3Mg/Fe sample dried at 393 K (a) and then calcined at 673 K (b).

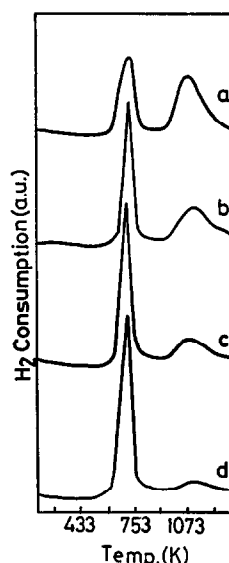


Fig. 6. TPR profiles for the (a) 2Mg/Fe, (b) 3Mg/Fe, (c) 6Mg/Fe and (d) 10Mg/Fe samples after calcination at 673 K.

0.67 mm/s. This may imply the decomposition of the HTLC structure and the formation of Fe–Mg mixed oxide upon calcination, consisting with the results of XRD and TG–DTA presented above.

In Fig. 6 the TPR profiles of the calcined Fe–Mg HTLC samples are shown. There are two peaks around 753 and 1173 K on each of these profiles, indicating two reduction stages for iron species. The relative areas of the second peak decreases with the increase of Mg/Fe ratios. The Mössbauer results revealed that the degree of reduction of iron species to Fe⁰ decreases with the increase of Mg/Fe ratios. These results suggest that the two reduction peaks on the TPR profiles correspond to the sequential

Table 2
Relative areas (%) of Mössbauer spectra of calcined Fe–MgHTLC samples reduced at 673 and 773 K

Sample	673 K			773 K		
	Fe ³⁺	Fe ²⁺	Fe ⁰	Fe ³⁺	Fe ²⁺	Fe ⁰
1Mg/Fe	0	62	38	0	40	60
3Mg/Fe	0	100	0	0	76	24
6Mg/Fe	36	64	0	0	75	25

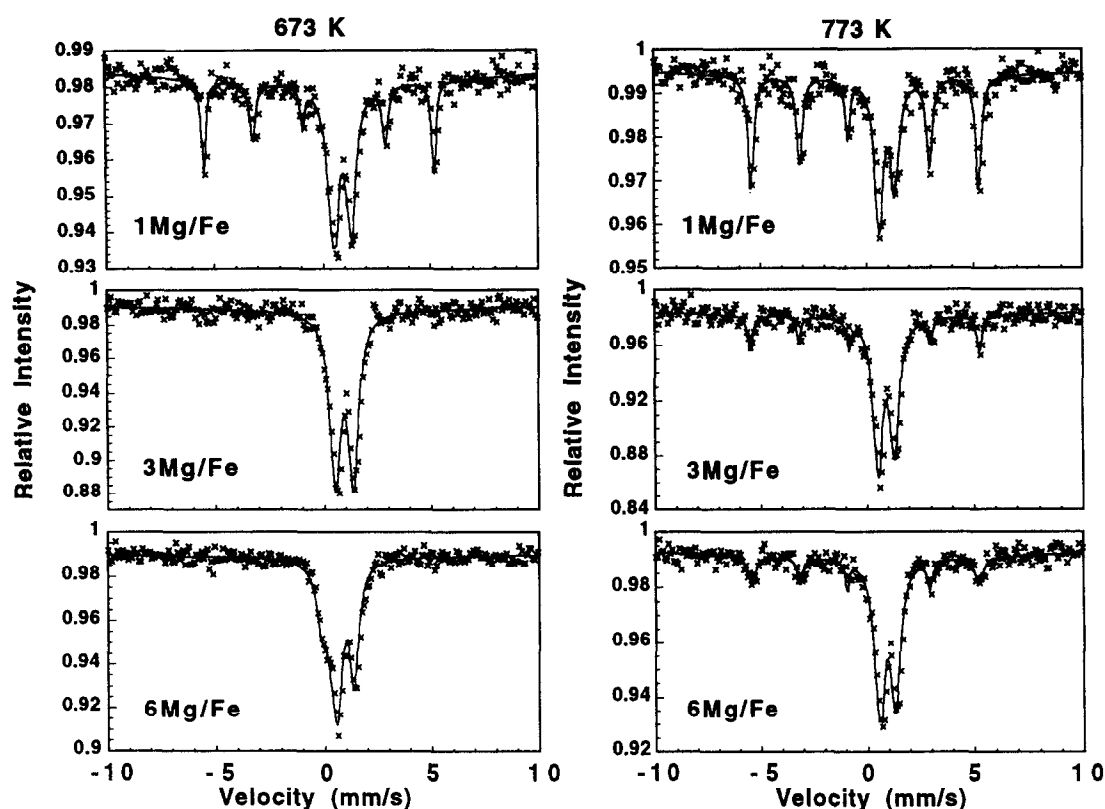


Fig. 7. Mössbauer spectra of the calcined Fe–Mg samples with different Mg/Fe ratios as indicated after reduction at 673 and 773 K, respectively.

reductions of iron species from Fe^{3+} to Fe^{2+} and then from Fe^{2+} to Fe^0 .

When Fe_2O_3 was treated in H_2 at 573 K, Fe_3O_4 was formed exclusively. Treatment of Fe_2O_3 in H_2 at 673 K resulted in the complete reduction of iron species to metallic iron.

Fig. 7 and Table 2 show the effect of coexisting Mg^{2+} on reducibility of iron species in calcined Fe–Mg HTLC samples. After being reduced at 673 K, the 1Mg/Fe sample exhibited 38% of Fe^0 and 62% of Fe^{2+} while the 3Mg/Fe sample exhibited 100% of Fe^{2+} . For

Table 3
Fischer–Tropsch reactivities of iron and iron–magnesium catalysts

Catalyst		Iron	1Mg/Fe	3Mg/Fe	6Mg/Fe
CO conversion (%)		96.7	82.2	24.3	17.8
CO ₂ formation (%) ^a		9.5	40.9	37.7	41.4
Hydrocarbon distribution (%)	C ₁	58.4	48.8	34.0	37.7
	C ₂	18.7	20.4	17.2	18.1
	C ₃	14.9	21.2	31.8	28.6
	C ₄	4.6	5.1	11.9	10.4
	C ₅	3.4	4.6	5.1	5.2
Olefin to paraffin ratio	C ₂ ⁼ /C ₂	0.009	0.07	0.44	0.98
	C ₃ ⁼ /C ₃	0.006	0.32	0.65	5.55
	C ₄ ⁼ /C ₄	0.25	0.11	0.55	0.42

^a CO₂ formation is defined as the percentage of CO converted to CO₂ in the total CO converted.

the 6Mg/Fe sample, only 36% of Fe^{3+} were reduced to Fe^{2+} at 673 K. Apparently, the coexistence of Mg^{2+} retarded the reduction of iron species. The same conclusion can be reached when the samples were reduced at 773 K.

Fischer–Tropsch reactions were performed for the catalysts obtained from the pure iron sample and from those Fe–Mg HTLC samples with different Mg/Fe ratios. Table 3 gives the results. The samples were pre-reduced in H_2 at 773 K for 4 h before the reactions. After the reduction, the pure iron catalyst had been reduced to α -Fe according to the Mössbauer results discussed above. The α -Fe were converted to iron carbide during the Fischer–Tropsch reaction [19]. This catalyst showed high activity with 97% CO conversion. With the increase of magnesium content in the catalysts, the Fischer–Tropsch activity decreased significantly with the decrease of amount of α -Fe formed in the catalysts reduced at 773 K. The production of methane decreased while the production of higher hydrocarbons (C_2 – C_5) and the olefin to paraffin ratio in the hydrocarbon products increased with the increase of magnesium content. This is probably due to the effect of strong basicity of MgO [20] in the catalysts which can act as a promoter of the electron donor. The most remarkable feature of the catalysts obtained from Fe–Mg HTLC for the Fischer–Tropsch reaction is the formation of CO_2 in great quantity. About 40% converted CO was converted to CO_2 on these catalysts, which may also be accounted by the strong basicity of MgO which may promote the water–gas shift reaction.

Acknowledgements

We acknowledge the financial supports from the Trans-Century Training Program Foundation for Talents by the State Education Commission of China and the National Natural Science Foundation of China.

References

- [1] R. Allmann, *Chimica*, 24 (1970) 99.
- [2] S. Miyata and A. Okada, *Clay Clay Miner.*, 25 (1977) 14.
- [3] W.T. Reichle, *Chemtech*, Jan. (1986) 58.
- [4] W.T. Reichle, *Solid States Ionics*, 22 (1986) 135.
- [5] C. Busetto, G. Del Piero, G. Manara, F. Trifiro and A. Vaccari, *J. Catal.*, 85 (1984) 260.
- [6] W.T. Reichle, *J. Catal.*, 94 (1985) 547.
- [7] W.T. Reichle, S.Y. Kang and D.S. Everhardt, *J. Catal.*, 101 (1986) 352.
- [8] S. Gusi, F. Pizzoli, F. Trifiro, A. Vaccari and G. Del Piero, *Prep. Catal. IV*, Elsevier Science, Amsterdam, 1987, p. 753.
- [9] G. Fornasari, S. Gusi, F. Trifiro and A. Vaccari, *Ind. Eng. Chem. Res.*, 26 (1987) 1500.
- [10] T. Yamaoka, M. Abe and M. Tsuji, *Mater. Res. Bull.*, 24 (1989) 1183.
- [11] H. Schaper, J.J. Berg-Slot and W.H.J. Stock, *Appl. Catal.*, 54 (1989) 79.
- [12] F. Cavani, F. Trifiro and F. Vaccari, *Catal. Today*, 11 (1991) 173.
- [13] O. Clause, B. Rebours, E. Merlen, F. Trifiro and A. Vaccari, *J. Catal.*, 133 (1992) 231.
- [14] A.L. McKenzie, C.T. Fishel and R.J. Davis, *J. Catal.*, 138 (1992) 547.
- [15] R.J. Davis and E.G. Derouane, *J. Catal.*, 132 (1991) 269.
- [16] A. Corma, V. Fornes, R.M. Martin-Aranda and F. Rey, *J. Catal.*, 134 (1992) 58.
- [17] K. Fuda, N. Kudo, S. Kawai and T. Matsunaga, *Chem. Lett.*, (1993) 777.
- [18] Jianyi Shen, J.M. Kobe, Yi Chen and J.A. Dumesic, *Langmuir*, 10 (1994) 3902.
- [19] J.A. Amelse, J.B. Butt and L.H. Schwartz, *J. Phys. Chem.*, 82 (1978) 558.
- [20] Jianyi Shen, R.D. Cortright, Yi Chen and J.A. Dumesic, *J. Phys. Chem.*, 98 (1994) 8067.